The Structure of the Active Site H-Cluster of [FeFe] Hydrogenase from the Green Alga Chlamydomonas reinhardtii Studied by X-ray Absorption Spectroscopy

ARTICLE *in* BIOCHEMISTRY · MAY 2009

Impact Factor: 3.02 · DOI: 10.1021/bi900010b · Source: PubMed

4 AUTHORS, INCLUDING:

Sven Timo Stripp
Freie Universität Berlin
18 PUBLICATIONS **514** CITATIONS
SEE PROFILE

Michael Haumann
Freie Universität Berlin
102 PUBLICATIONS **3,680** CITATIONS
SEE PROFILE

5042 *Biochemistry* **2009,** *48,* 5042–5049
DOI: 10.1021/bi900010b

BIOCHEMISTRY
including biophysical chemistry & molecular biology
Article

The Structure of the Active Site H-Cluster of [FeFe] Hydrogenase from the Green Alga *Chlamydomonas reinhardtii* Studied by X-ray Absorption Spectroscopy[†]

Sven Stripp,[‡,||] Oliver Sanganas,[§,||] Thomas Happe,*[,‡] and Michael Haumann*[,§]

[‡]*Lehrstuhl für Biochemie der Pflanzen, AG Photobiotechnologie, Ruhr-Universität Bochum, 44780 Bochum, Germany, and* [§]*Institut für Experimentalphysik, Freie Universität Berlin, Arnimallee 14, 14195 Berlin, Germany* [||] *These authors contributed equally to this work*

Received January 5, 2009; Revised Manuscript Received April 14, 2009

ABSTRACT: The [FeFe] hydrogenase (*Cr*HydA1) of the green alga *Chlamydomonas reinhardtii* is the smallest hydrogenase known and can be considered as a "minimal unit" for biological H_2 production. Due to the absence of additional FeS clusters as found in bacterial [FeFe] hydrogenases, it was possible to specifically study its catalytic iron−sulfur cluster (H-cluster) by X-ray absorption spectroscopy (XAS) at the Fe K-edge. The XAS analysis revealed that the *Cr*HydA1 H-cluster consists of a [4Fe4S] cluster and a diiron site, $2Fe_H$, which both are similar to their crystallographically characterized bacterial counterparts. Determination of the individual Fe−Fe distances in the [4Fe4S] cluster (~2.7 Å) and in the $2Fe_H$ unit (~2.5 Å) was achieved. Fe−C (=O/N) and Fe−S bond lengths were in good agreement with crystallographic data on bacterial enzymes. The loss of Fe−Fe distances in protein purified under mildly oxidizing conditions indicated partial degradation of the H-cluster. Bond length alterations detected after incubation of *Cr*HydA1 with CO and H_2 were related to structural and oxidation state changes at the catalytic Fe atoms, e.g., to the binding of an exogenous CO at $2Fe_H$ in CO-inhibited enzyme. Our XAS studies pave the way for the monitoring of atomic level structural changes at the H-cluster during H_2 catalysis.

Hydrogenases are efficient catalysts for the production and cleavage of molecular hydrogen (H_2) (*1*, *2*). Their use in biotechnological applications is expected to significantly contribute to future renewable fuel production (*3*, *4*). The molecular principles of H_2 turnover in these enzymes may lead to novel non-platinum catalysts (*5*). It is thus an important challenge to unravel the reaction mechanism of H_2 catalysis in hydrogenases.

In biocatalysis the [FeFe] hydrogenases are of particular interest as they show extremely high rates of H_2 production (*6*, *7*). The structures of [FeFe] hydrogenases from two bacterial species, namely, *Clostridium pasteurianum* and *Desulfovibrio desulfuricans*, have been resolved by protein crystallography (*8*, *9*). Their active site is a unique iron−sulfur cluster, comprising six Fe atoms commonly known as the H-cluster (*6*, *10*). It can be divided into a [4Fe4S] cluster and a binuclear iron unit, $2Fe_H$,[1] cysteine-linked to the cubane. This diiron moiety is probably the active site of H_2 catalysis (*8*, *11*, *12*). This situation differs from that in the [NiFe] hydrogenases where a heterobimetallic complex forms the active site (*13*). Depending on the redox conditions, the two Fe atoms of $2Fe_H$ bind three to four CO and two CN ligands. One CO may be found in an Fe−Fe bridging position (*14*−*17*). An azadithiolate (adt) moiety has been proposed, but the precise chemical identity of this ligand on top of the $2Fe_H$ site is not yet settled (*12*, *18*). Besides the H-cluster, bacterial [FeFe] hydrogenases harbor up to four additional FeS clusters, serving as electron transfer relays (*19*). Signal overlay from these clusters complicates investigations on the reaction cycle of the bacterial H-cluster by Fe-specific techniques, i.e., Mössbauer (*20*) and X-ray absorption spectroscopy (XAS) (*18*, *21*, *22*).

[FeFe] hydrogenases exist not only in anaerobic bacteria but also in photosynthetic eukaryotes. For several green algae, the *hydA* genes and respective proteins have been identified (*23*−*26*). These extraordinarily small proteins may be regarded as a "minimal unit" of biological H_2 conversion. Sequence alignments show that the small F-domain carrying the FeS relay clusters in bacteria is missing (*24*, *25*). However, four cysteine residues necessary for H-cluster accommodation in the H-domain are well conserved in all hydrogenase-coding *hydA* genes (*23*).

The biophysical characterization of algal [FeFe] hydrogenases is hampered by the fact that these enzymes are extremely O_2 sensitive and synthesized *in vivo* only in small amounts (*23*, *28*). To overcome low protein yields, we have established a general

[†]Financial support by the Deutsche Forschungsgemeinschaft (SFB498-C8, M.H.; SFB480, T.H.), the "Unicat" Cluster of Excellence Berlin, the Bundesministerium für Bildung and Forschung ($BioH_2$ program), and the EU/Energy Network SolarH2 (FP7 contract 212508) is gratefully acknowledged.

*Corresponding authors. T.H.: phone: +49 234 32 27026; fax: +49 234 32 14322; e-mail: thomas.happe@rub.de. M.H.: phone: +49 30 838 56101; fax: +49 30 838 56299; e-mail: michael.haumann@fu-berlin.de.

[1]Abbreviations: $2Fe_H$, binuclear Fe unit of the H-cluster; adt, azadithiolate; AI, as-isolated state; CpI, *Clostridium pasteurianum* [FeFe] hydrogenase; DdH, *Desulfovibrio desulfuricans* [FeFe] hydrogenase; EPR, electron paramagnetic resonance spectroscopy; EXAFS, extended X-ray absorption fine structure; FTIR, Fourier-transform infrared spectroscopy; *Cr*HydA1, [FeFe] hydrogenase protein of *C. reinhardtii*; MS, multiple scattering; XAS, X-ray absorption spectroscopy.

 Published on Web 04/14/2009

system for heterologous expression and synthesis of [FeFe] hydrogenases in *Clostridium acetobutylicum*. The [FeFe] hydrogenase from *Chlamydomonas reinhardtii*, *Cr*HydA1, is efficiently assembled due to the maturation apparatus of the host organism, yielding 2 mg of protein/L of cell culture (*28*). Hence, a sufficient amount of *Cr*HydA1 [FeFe] hydrogenase is available for in-depth spectroscopic explorations.

*Cr*HydA1 is an ideal candidate to study the assembly, structure, and catalytic mechanism of [FeFe] hydrogenases. First, EPR studies on *Cr*HydA1 and two further algal [FeFe] hydrogenases revealed similar signals of their CO-inhibited state of the active site as found in bacterial enzymes. However, deviations in the EPR *g*-tensors suggested distinct differences in the electronic structure of the H-cluster (*27*). Direct information on the geometric structure of the *Cr*HydA1 H-cluster is required to compare it to the situation in bacteria.

In the present study X-ray absorption spectroscopy (XAS) (*29*) at the Fe K-edge was performed to obtain atomic level structural and electronic information on the H-cluster of *Cr*HydA1. We show that the structural parameters imply an overall organization of the algal H-cluster similar to that in bacterial enzymes. Structural alterations induced by the inhibitor CO and the substrate H_2 are addressed.

MATERIALS AND METHODS

Protein Sample Preparation. C. reinhardtii [FeFe] hydrogenase *Cr*HydA1 was heterologously synthesized and isolated as previously described (*30*). *C. acetobutylicum* ATCC 824 recombinant strains were grown in CGM media containing up to 60 g/L glucose in a 2.5 L MiniFors bioreactor (Infors, Augsburg, Germany) (*28*, *31*). Both cell growth and protein purification were carried out under strictly anoxic conditions. Isolated protein was concentrated up to 1 mM (about 48 mg/mL) on Vivaspin 6 and Vivaspin 500 columns (Sartorius Stedim Biotech, Göttingen, Germany) and stored in 10% glycerol and 2 mM sodium dithionite (NaDT) for stabilization.

The specific H_2-evolving activity was determined by an *in vitro* assay as described before (*23*). The gas mixture was injected into a gas chromatograph (GC-2010; Shimadzu, Kyoto, Japan) equipped with a PLOT fused silica coating Molsieve column (5 Å, 10 m by 0.32 mm) from Varian (Palo Alto, CA). The specific activity of the hydrogenase was calculated from the detected amount of produced H_2.

For gas treatments, protein samples (~1 mM) were filled into open 200 μL PCR tubes and placed in 8 mL Suba tubes, which were rubber sealed under the N_2/H_2 atmosphere of the anaerobic tent. To humidify the working gases (CO, H_2), degassed water was bubbled with each of the two gases for 30 min, respectively. The headspace of the hermetically sealed Suba tubes was flushed with gas for 15−30 min. The final protein concentration of the samples used at the DESY Hamburg was adjusted right after the gas treatments; hence, more diluted protein was flushed. During the treatments, protein was kept on ice and protected against light. For the "as-isolated" samples (AI), no gas treatment was applied. Here, AI^{red} denotes an (optimal) enzyme isolation procedure in the presence of 2 mM NaDT, whereas AI^{ox} samples are preparations without any reducing agents (NaCl was used instead of NaDT to adjust the ionic strength of the buffers). Samples were filled into Kapton-covered acrylic-glass sample holders for XAS and frozen in liquid nitrogen. EPR measurements on the XAS samples (not shown) revealed no indications for significant unspecific iron in the as-isolated reduced *Cr*HydA1 samples as the "rhombic iron" signal at a *g*-value of ~4 was practically absent. The absence of water-dissolved Fe ions in as-isolated reduced *Cr*HydA1 samples was also likely according to the K-edge spectra, which showed no evidence for Fe−O bonds (see Results).

X-ray Absorption Spectroscopy (XAS). Kα fluorescence-detected XAS spectra at the Fe K-edge were collected at 20 K using energy-resolving Ge detectors and helium cryostats as previously described (*22*, *32*) at beamline D2 of the EMBL outstation (at HASYLAB, DESY, Hamburg, Germany) and at beamline KMC-1 of BESSY (Berlin, Germany). Harmonic rejection was achieved by detuning of the Si(111) double-crystal monochromators to 50% of their peak intensities. The energy resolution of the used monochromators was ~3 eV at DESY and optimized by appropriate setting of aperture slits and slightly lower, ~4 eV, at BESSY due to the beamline specifics (*33*). The slightly different energy resolution of the XAS spectra does not affect the conclusions drawn from the data analysis. Spectra were collected maximally for a scan range of 6950−8450 eV, i.e., up to k = 19.5 Å^{-1}, within ~1 h each. Dead time-corrected XAS spectra were averaged after energy calibration of each scan using the peak at 7112 eV in the first derivative of the absorption spectrum of an Fe foil as an energy standard (estimated accuracy ±0.1 eV) (*18*). EXAFS oscillations were normalized and extracted as described in refs *29* and *34*. The energy scale of EXAFS spectra was converted to the wave vector scale (k-scale) using an E_0 value of 7112 eV. Unfiltered k^3-weighted spectra were used for least-squares curve fitting employing a curved-wave multiple-scattering (MS) approach with the program EXCURV (*35*). In our hands, the EXCURV program is able to reproduce the expected coordination numbers of Fe−ligand interactions in Fe model compounds with known structure from fitting of respective EXAFS oscillations ranging up to k-values of 20 Å^{-1} (*18*). An amplitude reduction factor, S_0^2, of 0.9 was used in the EXAFS fits. EXAFS fits initially were based on a model of the H-cluster derived from the crystal structures (*8*, *9*). The CO and CN ligands were classified as units, with almost linear arrangement of the Fe−C=O/N atoms (bond angles close to 180°). For the units, correlation was enabled. A maximal path length in MS calculations of 10 Å and extending over a maximal scattering order of 4 was employed. Debye−Waller factors ($2\sigma^2$) were either fixed at physically reasonable values (see Table 2) or varied in the simulations. Fourier transforms (FTs) were calculated from k^3-weighted EXAFS data using the program SimX (*29*) and employing $\cos^2$ windows ranging over 10% at both ends of the k-range. From experimental K-edge spectra the preedge peak region was extracted by subtraction of a polynomial spline through the main edge rise using the program XANDA (*36*). K-edge energies were determined by the "integral method" (*29*), using integration limits of 15% and 90% of normalized intensity.

RESULTS

As-Isolated Reduced State of CrHydA1. Purification of the protein under strictly anaerobic and reducing conditions (*30*) to obtain the as-isolated state of *Cr*HydA1 (AI^{red}) yielded the most active protein (Table 1). Iron XAS spectra of AI^{red} were collected up to a k-value of 19.5 Å^{-1}, i.e., to ~1450 eV above the Fe K-edge at ~7120 eV (Figure 1). This very long k-range for XAS on proteins allows for resolution even of closely spaced interatomic distances (*34*, *37*).

Table 1: Specific H_2-Evolving Activities of *Cr*HydA1 Preparations

sample	specific H_2 evolving activity (μmol of H_2 mg^{-1} min^{-1}) ± 20
*Cr*HydA1^{red}	650
*Cr*HydA1^{ox}	590
H_2 treated	620
CO treated	40

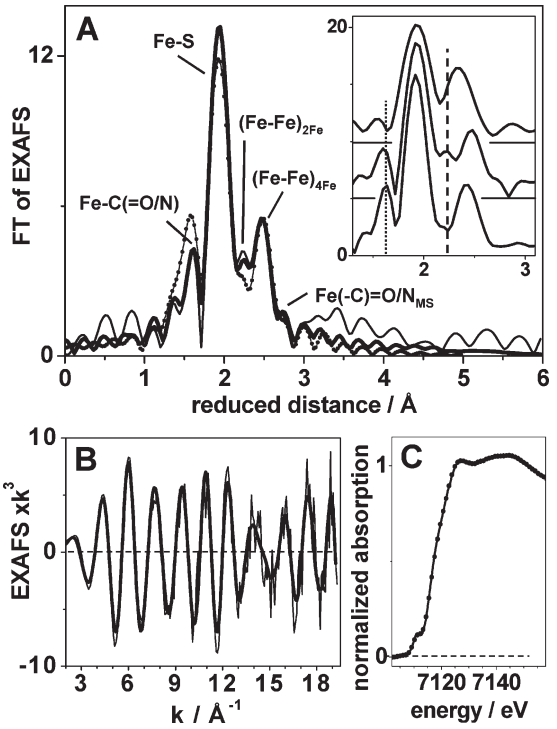

FIGURE 1: XAS analysis of as-isolated reduced *Cr*HydA1 (AI^{red}) at the Fe K-edge. (A) Fourier transform of the EXAFS spectrum in (B). The FT was calculated from *k*-values ranging over 4.7−19.5 $Å^{-1}$. Inset: FTs calculated from *k*-ranges starting at 7.4, 4.9, and 1.6 $Å^{-1}$ (top to bottom); vertical lines mark contributions from Fe−C(=O/N) vectors (dots) and from the Fe−Fe vector in $2Fe_H$ (dashes). (A) and (B): thin lines, experimental data; thick lines, simulations (Table 2C); the dotted line in (A) is a simulation with parameters in Table 2A. (C) Fe K-edge spectra of two AI^{red} preparations measured at DESY (line) and BESSY (dots).

The K-edge spectrum of AI^{red} (Figure 1C) was perfectly reproducible in independent protein samples, indicating the high quality of the *Cr*HydA1 preparation. Its small primary maximum at ~7130 eV revealed the predominant coordination of Fe by sulfur ligands (*22*, *38*) as expected due to the presence of the respective conserved cysteines in *Cr*HydA1. Indications for oxygen ligation of Fe, as expected for oxidatively modified (or damaged) FeS species (*22*), were absent.

The Fourier transform (FT) of the AI^{red} EXAFS spectrum shows three major peaks (Figure 1A), at reduced distances between ~1.5 and ~2.5 Å (the reduced distance is the true interatomic distance minus ~0.4 Å due to a phase shift). This immediately suggests at least three Fe−backscatterer shells, i.e., of Fe−C(=O/N), Fe−S, and Fe−Fe vectors. A shoulder on the high-distance side of the FT peak due to Fe−Fe interactions likely accounted for the expected Fe(C)=O/N interactions, the contributions of which to the EXAFS spectrum usually are enhanced by multiple scattering (MS) effects due to the almost linear Fe−C=O/N arrangement (see below). The FT peaks due to Fe−C(=O/N) and Fe(−C)=O/N interactions may be expected to be similarly large (*18*). Here, the magnitude of the peak due to Fe(−C)=O/N apparently was diminished due to partial cancelation of respective EXAFS oscillations by interference with EXAFS contributions from the Fe−Fe interactions. A fourth peak at ~2.2 Å reduced distance became more prominent when the FT was calculated starting at higher *k*-values (Figure 1A, inset) where metal−metal interactions dominate the EXAFS oscillations (shown in Figure 1B). This result was suggestive of a Fe−Fe distance of 2.5−2.6 Å in the H-cluster. The Fe−Fe distance of the $2Fe_H$ unit in crystal structures of bacterial [FeFe] hydrogenases is about 2.5 Å, whereas the Fe−Fe distances in the [4Fe4S] cluster are ~2.7 Å (*8*, *9*). Thus, the EXAFS data apparently allow to discriminate between the Fe−Fe distances in the [4Fe4S] and the $2Fe_H$ subgroups of the *C. reinhardtii* H-cluster.

Precise Fe−ligand distances in AI^{red} were determined by simulations (curve fitting) of the EXAFS spectrum. We used a multiple scattering (MS) approach (*35*, *39*) to account for the expected (relatively small) MS contributions to the EXAFS from the linear CO and CN ligands at $2Fe_H$. It should be noted that very similar fit results with respect to bond lengths and coordination numbers were obtained if MS contributions very neglected in the simulation procedure (not documented). First, coordination numbers were employed in the simulations (Table 2) which where based on the crystal structures of the H-cluster in bacterial [FeFe] hydrogenases (*8*, *9*, *14*). Possible weak Fe−Fe interactions between the two parts of the H-cluster were neglected in the simulations as all distances between Fe ions of the [4Fe4S] cluster and of $2Fe_H$ are ≥4 Å in crystal structures of the bacterial enzymes and such interactions did not contribute significantly to the EXAFS spectra. The fit results in Table 2A and the corresponding fit curve (Figure 1A, dotted line) revealed that the main features of the EXAFS spectrum already were reasonably well reproduced by using the crystal structure as a template. All Fe−ligand distances, in particular the two Fe−Fe and Fe−S distances (Table 2A), are similar to those found in the crystal structures of *Cp*I and *Dd*H (*8*, *9*). Sequence similarity of the catalytic H-domain of these bacterial hydrogenases to *Cr*HydA1 is reasonable high. Still, structures derived from X-ray crystallography, especially for metal cofactors, have to be considered with care. The good agreement of XAS analysis and crystal structure, however, suggests that the overall organization of the green algae H-cluster is similar to that of bacteria.

A more elaborated fit approach yielded refined structural parameters of the H-cluster. Allowing the coordination numbers (N_i) of the Fe−C(=O/N) and Fe−Fe distances to vary in the fit yielded a lower $N_{Fe-C(=O/N)}$ value but a larger *N*-value of the ~2.5 Å Fe−Fe distance (Table 2B). An $N_{Fe-C(=O/N)}$ value of less than unity, i.e., less than one C(=O/N) ligand per each of the six Fe atoms on the average, was expected for the absence of a CO in a bridging position between the two iron atoms of $2Fe_H$. In the literature, the reduced form of the H-cluster (H_{red}) has been reported to lack this bridging CO, and the respective CO group is bound to Fe_p (p = proximal) solely. Upon oxidation, the CO bridge between the distal and proximal Fe atoms is formed (*14*, *16*, *17*, *41*−*43*). The as-isolated AI^{red} protein of *Cr*HydA1 from our preparations is not likely to contain oxidized or CO-inhibited impurities. Due to our fast and gentle isolation protocol, EPR spectra of AI^{red} did not show the axial EPR signal with *g*-values of 2.102, 2.040, and 1.998 as expected for *Cr*HydA1^{ox} and 2.052, 2.007, and 2.007 for *Cr*HydA1^{ox}-CO as reported recently (*27*). Roseboom et al. explained the frequent

emergence of CO-inhibited species by cannibalization of free CO from denatured protein (*17*). However, these impurities were not detected in AI^{red}. A larger apparent coordination number than the expected one of 0.33 (due to two Fe−Fe distances of ~2.5 Å per six Fe ions) of the Fe−Fe distance attributed to $2Fe_H$ may suggest contributions from similarly long Fe−S vectors. In the structure of reduced [FeFe] hydrogenase from *C. pasteurianum* the distance of Fe_p at the $2Fe_H$ site to the cysteine sulfur atom which links it to the [4Fe4S] cluster is ~2.50 Å, and the Fe−Fe distance in $2Fe_H$ is only slightly longer, ~2.55 Å. Thus, such a long Fe−S distance may contribute to the apparent coordination number of the Fe−Fe interaction. We note that in the crystal structures all further Fe−S bonds are shorter than about 2.4 Å, and such distances would not interfere with the 2.5 Å feature.

The coordination number of the Fe−Fe distance of ~2.7 Å ($N_{2.7}$) was very close to 2 (2.02) if it was allowed to vary in the fit (Table 2). This value is similar to the one of 2.0 that is calculated for the presence of only the H-cluster in *Cr*HydA1 (i.e., for 12 Fe−Fe distances of ~2.7 Å in the cubane moiety per 6 Fe ions). In the [FeFe] hydrogenases of *Cp*I and *Dd*H, besides the H-cluster, four and two additional FeS clusters are found so that the $N_{2.7}$ values would be expected to be significantly larger, 2.27 and 2.52, respectively. Thus, our XAS data suggest, in concert with previously performed EPR experiments (*27*, *30*) and multiple sequence alignments (*23*−*25*), that only the H-cluster is present in *Cr*HydA1 and further FeS clusters are absent.

A significant further improvement of the fit quality (R_F less than 10%) was achieved by including separate shells for the Fe−C(=O) and Fe−C(=N) interactions and further slight parameter adjustments (Table 2C; Figure 1A,B, thick lines). Now, individual distances for Fe−C(=O) of 1.77 Å and Fe−C (=N) of 1.98 Å were obtained. These distances are close to those of the respective ligands in the crystal structures, where the Fe−C (=O) distance usually is shorter than Fe−C(=N) (*8*, *9*).

We note that the above used "top-down" simulation approach, i.e., starting the EXAFS simulations with a model based on the crystal structures of the H-cluster in bacteria and then refining the structural parameters by additional degrees of freedom in the fit, leads to the same simulation results that were obtained by an inverse ("bottom-up") procedure where the structural model was developed by the stepwise inclusion of increasing numbers of coordination shells in the fit (not documented).

An unusual bridging ligand (which perhaps is an azadithiolate (adt)) has been proposed to be present in the $2Fe_H$ part of the bacterial H-cluster and may serve crucial functions in H_2 production (*9*, *14*, *44*−*47*). The respective carbon and nitrogen or oxygen atoms would be within a range of about 3−4 Å to the Fe atoms of $2Fe_H$. As such distances overlap with those from Fe (−C)=O/N interactions and only weak contributions from these atoms to the EXAFS spectra were expected, the nature of the bridging species in the *C. reinhardtii* H-cluster cannot be deduced from the XAS data.

H-Cluster Integrity in Protein from Two Purification Conditions. The integrity of the active site was compared in as-isolated *Cr*HydA1 samples purified under reducing (AI^{red}) and mildly oxidizing (AI^{ox}) conditions (Figure 2). The specific H_2-evolving activity of AI^{ox} samples, as determined by the *in vitro* assay, was only slightly lower than in AI^{red} (Table 1). The Fe K-edge was at ~0.5 eV higher energies in AI^{ox} compared to AI^{red} (Figure 2A), indicating that overall more reduced Fe was present in AI^{red}. Both K-edges were at higher energies than that for Fe(II) species due to the presence of Fe(III) ions in the cubane cluster (*48*, *49*). The shift of the edge to lower energies in AI^{red} was compatible with the reduction of at least one Fe(III) ion to the Fe(II) state. Furthermore, the preedge peak, due to formally dipole-forbidden 1s → 3d electronic transitions, was increased in AI^{ox} (Figure 2A, inset). This suggests a less symmetric overall Fe coordination (*40*), presumably due to the binding of oxygen species to some Fe atoms in AI^{ox} (see below). Lowering of the site symmetry is expected to cause increased admixtures of metal p levels to the 3d electronic orbitals, increasing the probability of electronic transitions into unoccupied 3d levels and thus the intensity of the respective preedge feature. Due to the limited energy resolution of the monochromator at BESSY, possible spectral substructure on the preedge peaks, as related, i.e., to electronic multiplet interactions (*40*, *50*), remained invisible.

The FTs of EXAFS spectra revealed a pronounced decrease of the peak due to Fe−Fe interactions in AI^{ox} (Figure 2B, arrow). EXAFS simulations (using a simplified approach) revealed a

Table 2: Structural Parameters of the H-Cluster from EXAFS Simulations[a]

sample	shell	fit	N_i (per Fe)	R_i (Å)	$2\sigma_i^2$ (Å^2)	R_F (%)
AI^{red}	C(=O/N)	A	1.00[b]	1.78	0.002[b]	22.5
	S		2.17[d]	2.28	0.001[c]	
	S		1.33[d]	2.39	0.001[c]	
	Fe ($2Fe_H$)		0.33[b]	2.52	0.002[b]	
	Fe (4Fe4S)		2.00[b]	2.73	0.009	
	C(=O/N)	B	0.52	1.77	0.002[b]	21.0
	S		2.56	2.29	0.002[b]	
	S		1.14	2.40	0.002[b]	
	Fe ($2Fe_H$)		0.61	2.53	0.002[b]	
	Fe (4Fe4S)		2.02	2.71	0.010	
	C(=O)	C	0.45[e]	1.77	0.001[b]	8.7
	C(=N)		0.55[e]	1.98	0.001[b]	
	S		2.04[d]	2.28	0.001[b]	
	S		1.46[d]	2.40	0.003[b]	
	Fe ($2Fe_H$)		0.77	2.53	0.002[b]	
	Fe (4Fe4S)		2.02	2.72	0.012	
AI^{ox}	C(=O/N)	D	0.55	1.84	0.001[b]	7.7
(AI^{red})			(0.74)	(1.86)	(0.001)[b]	
	S		2.96	2.28	0.010[b]	
			(3.57)	(2.28)	(0.010)[b]	
	Fe ($2Fe_H$)		0.58	2.52	0.001[b]	
			(0.71)	(2.53)	(0.001)[b]	
	Fe (4Fe4S)		1.19	2.70	0.010[b]	
			(2.06)	(2.73)	(0.010)[b]	
AI^{red}	C(=O/N)	E	0.68	1.85	0.001[b]	8.3
[CO]			[0.92]	[1.79]	[0.001][b]	
{H_2}			{0.42}	{1.78}	{0.001}[b]	
	S		3.45[f]	2.29	0.010[b]	
			[3.45][f]	[2.27]	[0.010][b]	
			{3.45}[f]	{2.25}	{0.010}[b]	
	Fe ($2Fe_H$)		0.54[f]	2.53	0.002[b]	
			[0.54][f]	[2.62]	[0.002][b]	
			{0.54}[f]	{2.51}	{0.002}[b]	
	Fe (4Fe4S)		2.02[f]	2.73	0.012[b]	
			[2.02][f]	[2.71]	[0.012][b]	
			{2.02[f]}	{2.71}	{0.012}[b]	

[a] N_i, coordination number; R_i, Fe−ligand distance; $2\sigma_i^2$, Debye−Waller factor. [b] Fixed values. [c] $2\sigma^2$ restricted to values >0. [d] The sum of N_S values was 3.5. [e] The sum of $N_{C(=O/N)}$ values was 1. [f] N_i was coupled to yield equal values for the three spectra. R_F (*29*) was calculated over reduced distances of 1.3−2.8 Å. All simulations comprise a further multiple-scattering Fe(−C)=O/N shell (with the same N value as for the Fe−C (=O/N) shell; respective distances were in the range of 2.95−3.02 Å; $2\sigma^2$ was set to 0.01 Å^2).

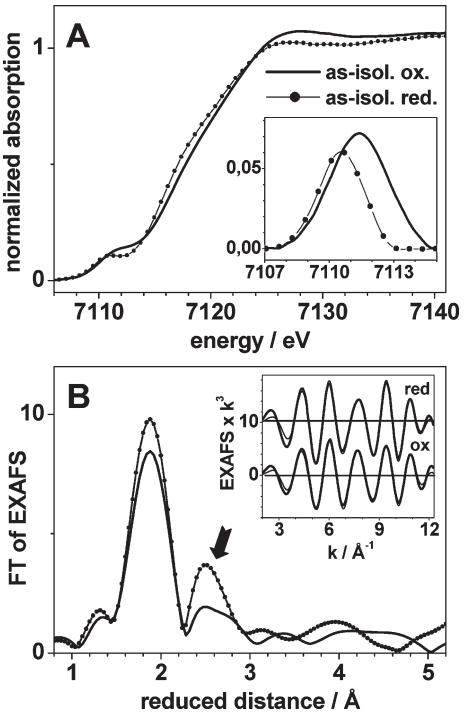

FIGURE 2: XAS comparison of as-isolated reduced (AI^{red}) and oxidized (AI^{ox}) *Cr*HydA1. (A) K-edge spectra (inset, isolated preedge features). (B) FTs of EXAFS spectra (dotted line, AI^{red}; solid line, AI^{ox}). FTs were calculated over a *k*-range of 1.6−12.5 Å^{-1}; the arrow marks the contributions mainly from Fe−Fe interactions. Inset: Fourier isolates over reduced distances of 0.5−3.0 Å (thin lines, experimental data) and simulations according to Table 2D (thick lines).

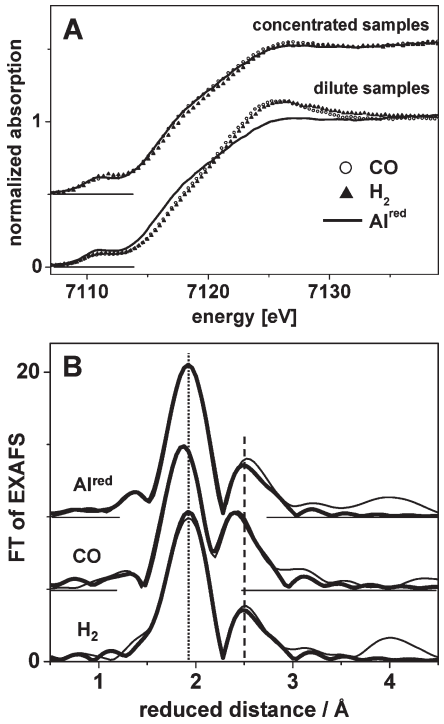

FIGURE 3: Effects of gas treatment on *Cr*HydA1: CO binding and H_2 reduction. (A) K-edges of indicated *Cr*HydA1 samples. (B) FTs of EXAFS spectra (thin lines, calculated as in Figure 2) and simulations (thick lines, Table 2E). H_2 and CO treatments in (B) were carried out on concentrated protein. Vertical dashed and dotted lines mark shifts in the respective FT peaks due to Fe−S and Fe−Fe interactions.

decrease of the coordination number of ~2.7 Å Fe−Fe vectors by a factor of about 2 and a less pronounced decrease of N_{Fe-S} and $N_{FeC(=O/N)}$. The *N*-value of the ~2.5 Å Fe−Fe distance in $2Fe_H$ of AI^{ox}, however, was only slightly smaller than that of AI^{red} (Table 2D). These results may suggest that in AI^{ox} primarily the [4Fe4S] part of the H-cluster was modified or destroyed, whereas in the larger protein fraction the binuclear site at least still contained the ~2.5 Å Fe−Fe distance. Whether this Fe−Fe distance belongs to an otherwise unmodified $2Fe_H$ cluster cannot be concluded from the data.

Effects of Treatments with CO and H_2. The effects of incubation of *Cr*HydA1 with CO and H_2 on the structure of the H-cluster strongly depended on whether concentrated or more dilute protein samples were treated (Figure 3). In diluted samples (Figure 3A), the increased primary maxima of the K-edges (at ~7125 eV) and lowered preedge amplitudes (at ~7111 eV) suggested overall more symmetric coordination of the Fe atoms. Such an effect was expected if Fe ions had become released from the protein to the medium, forming hexaquo−Fe ions. Such deleterious effects in dilute samples were observed with both gases. Analysis of the EXAFS data of H_2- and CO-treated dilute protein (not documented) revealed the partial loss of Fe−Fe interactions, which indicates a degradation of the H-cluster.

H_2 and CO treatments on more concentrated samples caused only small changes of the K-edge spectra (Figure 3A), suggesting that the integrity of the H-cluster was fully preserved. A slight shift of the edge to higher energies (by ~0.4 eV) in H_2-treated *Cr*HydA1 points to the oxidation of one Fe atom at $2Fe_H$, possibly due to reduction of H-species (*8*, *18*). The respective EXAFS spectrum (Figure 3B) showed only minor changes compared to AI^{red}. The main difference in the structure of the H-cluster, according to EXAFS simulations (Table 2E), was a decreased apparent Fe−C(=O/N) distance and a slightly decreased Fe−Fe distance of $2Fe_H$ in H_2-treated enzyme. Although this small decrease in the Fe−Fe distance may not be significant, it could be caused by the presence of one more oxidized Fe atom (likely Fe_d of $2Fe_H$; d = distal) due to the binding and reduction of H-species. Notably, the Fe−Fe distance of the [4Fe4S] cluster was not affected by the H_2 treatment (Table 2E).

Carbon monoxide is an effective inhibitor of [FeFe] hydrogenases. In a crystallographic structure for H_{ox}−CO of *Cp*I, electron density at Fe_d was discussed to be exogenous CO (*41*). FTIR and EPR analyses support this notion (*14*, *51*). Under certain redox conditions, an endogenous CO is believed to form a "bridge" between the Fe atoms of the $2Fe_H$ moiety (*6*, *41*). A decreased preedge peak in CO-treated *Cr*HydA1 (Figure 3A) was in agreement with an overall more symmetric Fe coordination upon binding of additional CO to $2Fe_H$. The EXAFS data (Figure 3B) revealed an increased coordination number of the Fe−C(=O/N) interactions accompanied by enhanced respective multiple scattering contributions to the spectrum and an overall reduced mean FeC(=O/N) distance (Table 2E). These findings indicate the presence of one to two surplus short Fe−C(=O) interactions. In comparison to AI^{red}, the Fe−Fe distance of $2Fe_H$ was increased significantly by ~0.1 Å. A similar increase of the Fe−Fe distance has been observed in crystal structures of CO-treated bacterial [FeFe] hydrogenase, where one extra CO was found at Fe_d (*41*). Presumably, in *Cr*HydA1 an extra CO also was bound to Fe_d, causing more symmetric (near-octahedral) coordination of this ion.

DISCUSSION

XAS on biological metal centers (BioXAS) is a powerful tool to derive atomic resolution structural information, to determine the electronic configuration, especially in those states which are not accessible by EPR spectroscopy, and to monitor their dynamics during the catalytic reactions (*29*, *52*−*55*). Here, we used XAS at the Fe K-edge to specifically investigate the catalytic cofactor of biological H_2 turnover in an [FeFe] hydrogenase protein.

The structural parameters from the present XAS study strongly suggest that the overall atomic organization of the H-cluster in the [FeFe] hydrogenase of the green alga *C. reinhardtii* is very similar to that found in crystallographically characterized enzymes from bacteria. Recent EPR investigations performed on *Cr*HydA1 support this notion (*27*, *30*). Furthermore, the XAS data strongly suggest that in *Cr*HydA1 no additional FeS clusters are found, as opposed to bacterial hydrogenases (*2*, *8*, *9*). EXAFS analysis allowed precise determination of interatomic distances in the H-cluster. The individual Fe−Fe distances in the [4Fe4S] part and $2Fe_H$ moiety of the H-cluster were measured (precision on the order of ∼0.02 Å). Changes of the structural parameters upon treatments of *Cr*HydA1 with the inhibitor CO and the substrate H_2 were detected, allowing to address changes, e.g., in catalytic intermediates. The XAS-derived interatomic distances, because of their higher resolution compared to protein crystallography (*56*), may help to optimize *in silico* structures of the H-cluster in DFT calculations (*57*−*59*).

There are also limitations of the XAS analysis. By the applied methods, predominantly average coordination environments of the six Fe atoms in the cluster were obtained. Characterization of the individual structure and oxidation state of the Fe atoms, in particular in the $2Fe_H$ unit, and of the binding sites of substrate and inhibitors is highly desirable. It may be facilitated by future investigations employing site-selective XAS techniques (*60*). It has been proposed that an azadithiolate is bridging the Fe atoms of the $2Fe_H$ site and is essential in H_2 turnover (*12*, *18*, *45*−*47*, *61*). The respective C, N, and O atoms are almost impossible to detect by XAS because their distances to Fe are relatively large and overlap with the Fe(C)=O/N distances and with contributions of atoms from the protein backbone. Thus, discrimination between different bridging species likely cannot be obtained by XAS.

The integrity of the algal H-cluster is easily perturbed, as observed for *Cr*HydA1 purified under mildly oxidizing conditions and upon incubation of dilute protein with H_2 and CO. Such conditions seem to cause the release of Fe ions from the protein into the medium and, hence, at least partial degradation of the H-cluster. Preliminary evidence was obtained that the [4Fe4S] cluster is the primary target of oxidative modification, whereas the $2Fe_H$ moiety may be more robust. O_2 sensitivity of FeS clusters is well-known (*62*, *63*). Purification of *Cr*HydA1 under reducing conditions prevents such deleterious effects and stabilizes an intact H-cluster. In bacterial [FeFe] hydrogenases, the H-cluster is deeply buried in the protein. Induced-fit folding models of *Cr*HydA1 (M. Winkler and T. Happe, unpublished results) suggest that its [4Fe4S] cluster is located just beneath the surface whereas the $2Fe_H$ moiety faces the inside of the protein. This arrangement is likely to allow for easy access of gas molecules and redox partners from the bulk to the [4Fe4S] unit and for its rapid modification by O_2.

Treatments of *Cr*HydA1 with H_2 and CO revealed relatively subtle but discernible structural changes of the H-cluster. Interaction of the substrate H_2 with $2Fe_H$ seems to cause slight overall oxidation of the two Fe atoms in the $2Fe_H$ part, but its Fe−Fe distance was almost unchanged. Accordingly, a change in the Fe−Fe bridging motif upon H_2 binding, compared to reduced as-isolated *Cr*HydA1, is unlikely. If H-species become bound to $2Fe_H$, they may be located in a terminal position on Fe_d but not in an Fe−Fe bridging position. Further investigations are required to clarify this issue. CO binding to $2Fe_H$, on the other hand, caused a significant elongation of the Fe−Fe distance, and additional short Fe−C(=O) distances were found. These results are comparable with crystal data of CO-treated bacterial [FeFe] hydrogenases (*41*) and previous EPR data on *Cr*HydA1 (*27*). Presumably, the extra CO on Fe_d inhibits *Cr*HydA1 by causing a structural rearrangement, which blocks a binding site for H-species, in a similar fashion to that proposed for bacterial enzymes (*10*, *11*, *41*).

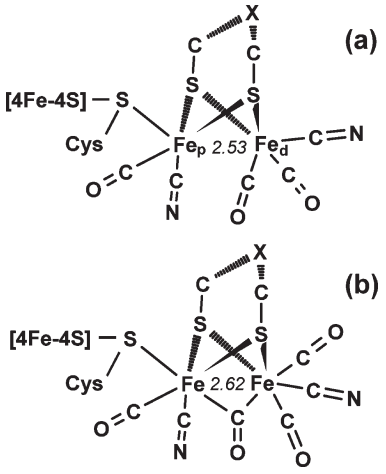

FIGURE 4: Tentative structures of the H-cluster in *Cr*HydA1 for AI^{red} and AI^{ox} CO. (a) As-isolated reduced and (b) CO-treated protein, in agreement with the XAS results (Fe−Fe distances in Å). The bridging ligand on top of the $2Fe_H$ cluster is (partly) visible in the crystal structures of bacterial [FeFe] hydrogenases (*8*−*12*). Its chemical nature, however, is unclear (X may be N or O). The respective C and N or O atoms were not resolved in this XAS study.

In conclusion, we show that by XAS on algal [FeFe] hydrogenase the site geometry and electronic configuration of the H-cluster can be resolved. It is possible to monitor changes upon substrate and inhibitor binding. For the first time, the bond lengths and Fe−Fe distances of the H-cluster were determined at subangstrom resolution. We summarize our results on the structure of the H-cluster in as-isolated reduced and CO-treated *Cr*HydA1 in the tentative models shown in Figure 4. Further investigations to characterize the active site of *C. reinhardtii* [FeFe] hydrogenase in its H_2 turnover cycle are in progress in our laboratories.

ACKNOWLEDGMENT

We thank the beamline scientists Dr. W. Meyer-Klaucke (EMBL at DESY, Hamburg) and Dr. F. Schäfers and M. Mertin (BESSY, Berlin) for excellent technical support and Prof. Holger Dau (FU-Berlin) for providing kind access to XAS measuring equipment at BESSY.

REFERENCES

1. Cammack, R., Robson, R., and Frey, M., Eds. (1997) *Hydrogen as a fuel: Learning from nature*, Taylor and Francis, London, U.K.

2. Vignais, P. M., and Billoud, B. (2007) Occurrence, classification, and biological function of hydrogenases: An overview. *Chem. Rev. 107*, 4206–4272.
3. Mertens, A., and Liese, A. (2004) Biotechnological applications of hydrogenases. *Curr. Opin. Biotechnol. 15*, 343–348.
4. Rittmann, B. E. (2008) Opportunities for renewable bioenergy using microorganisms. *Biotechnol. Bioeng. 100*, 203–212.
5. Evans, D. J., and Pickett, C. J. (2003) Chemistry and the hydrogenases. *Chem. Soc. Rev. 32*, 268–275.
6. Adams, M. W. W. (1990) The structure and mechanism of iron-hydrogenases. *Biochim. Biophys. Acta 1020*, 115–145.
7. Frey, M. (2002) Hydrogenases: hydrogen-activating enzymes. *ChemBioChem 3*, 153–160.
8. Peters, J. W., Lanzilotta, W. N., Lemon, B., and Seefeldt, L. C. (1998) X-ray crystal structure of the Fe-only hydrogenase (CpI) from *Clostridium pasteurianum* to 1.8 Å resolution. *Science 282*, 1853–1858.
9. Nicolet, Y., Piras, C., Legrand, P., Hatchikian, C. E., and Fontecilla-Camps, J. C. (1999) *Desulfovibrio desulfuricans* iron hydrogenase: the structure shows unusual coordination to an active site Fe binuclear center. *Struct. Folding Des. 7*, 13–23.
10. Peters, J. W. (1999) Structure and mechanism of iron-only hydrogenases. *Curr. Opin. Struct. Biol. 9*, 670–676.
11. Nicolet, Y., Cavazza, C., and Fontecilla-Camps, J. C. (2002) Fe-only hydrogenases: structure, function and evolution. *J. Inorg. Biochem. 91*, 1–8.
12. Nicolet, Y., Lemon, B. J., Fontecilla-Camps, J. C., and Peters, J. W. (2000) A novel FeS cluster in Fe only hydrogenases. *Trends Biochem. Sci. 25*, 138–143.
13. Volbeda, A., Charon, M. H., Piras, C., Hatchikian, E. C., Frey, M., and Fontecilla-Camps, J. C. (1995) Crystal structure of the nickel-iron hydrogenase from *Desulfovibrio gigas*. *Nature (London) 373*, 580–587.
14. Nicolet, Y., de Lacey, A. L., Vernède, X., Fernandez, V. M., Hatchikian, E. C., and Fontecilla-Camps, J. C. (2001) Crystallographic and FTIR spectroscopic evidence of changes in Fe coordination upon reduction of the active site of the Fe-only hydrogenase from *Desulfovibrio desulfuricans*. *J. Am. Chem. Soc. 123*, 1596–1601.
15. Chen, Z., Lemon, B. J., Huang, S., Swartz, D. J., Peters, J. W., and Bagley, K. A. (2002) Infrared studies of the CO-inhibited form of the Fe-only hydrogenase from *Clostridium pasteurianum* I: examination of its light sensitivity at cryogenic temperatures. *Biochemistry 41*, 2036–2043.
16. Pierik, A. J., Hulstein, M., Hagen, W. R., and Albracht, S. P. (1998) A low-spin iron with CN and CO as intrinsic ligands forms the core of the active site in [Fe]-hydrogenases. *Eur. J. Biochem. 258*, 572–578.
17. Roseboom, W., De Lacey, A. L., Fernandez, V. M., Hatchikian, E. C., and Albracht, S. P. J. (2006) The active site of the [FeFe]-hydrogenase from *Desulfovibrio desulfuricans*. II. Redox properties, light sensivity and CO-ligand exchange as observed by infrared spectroscopy. *J. Biol. Inorg. Chem. 11*, 102–118.
18. Löscher, S., Schwartz, L., Stein, M., Ott, S., and Haumann, M. (2007) Facilitated hydride binding in an Fe-Fe hydrogenase active-site biomimic revealed by X-ray absorption spectroscopy and DFT calculations. *Inorg. Chem. 46*, 11094–11105.
19. Fontecilla-Camps, J. C., Volbeda, A., Cavazza, C., and Nicolet, Y. (2007) Structure/function relationships of [NiFe]- and [FeFe]-hydrogenases. *Chem. Rev. 107*, 4273–4303.
20. Pereira, A. S., Tavares, P., Moura, I., Moura, J. J., and Huynh, B. H. (2001) Mössbauer characterization of the iron-sulfur clusters in *Desulfovibrio vulgaris* hydrogenase. *J. Am. Chem. Soc. 123*, 2771–2782.
21. Schwab, D. E., Tard, C., Brecht, E., Peters, J. W., Pickett, C. J., and Szilagyi, R. K. (2006) On the electronic structure of the hydrogenase H-cluster. *Chem. Commun. 35*, 3696–3698.
22. Buhrke, T., Löscher, S., Lenz, O., Schlodder, E., Zebger, I., Andersen, L. K., Hildebrandt, P., Meyer-Klaucke, W., Dau, H., Friedrich, B., and Haumann, M. (2005) Reduction of unusual iron-sulfur clusters in the H_2-sensing regulatory Ni-Fe hydrogenase from *Ralstonia eutropha* H16. *J. Biol. Chem. 280*, 19488–19495.
23. Happe, T., and Naber, J. D. (1993) Isolation, characterization and N-terminal amino acid sequence of hydrogenase from the green alga *Chlamydomonas reinhardtii*. *Eur. J. Biochem. 214*, 475–481.
24. Happe, T., and Kaminski, A. (2002) Differential regulation of the Fe-hydrogenase during anaerobic adaptation in the green alga *Chlamydomonas reinhardtii*. *Eur. J. Biochem. 269*, 1022–1032.
25. Winkler, M., Heil, B., Heil, B., and Happe, T. (2002) Isolation and molecular characterization of the [Fe]-hydrogenase from the unicellular green alga *Chlorella fusca*. *Biochim. Biophys. Acta 1576*, 330–334.
26. Florin, L., Tsokoglou, A., and Happe, T. (2001) A novel type of Fe-hydrogenase in the green alga *Scenedesmus obliquus* is linked to the photosynthetic electron transport chain. *J. Biol. Chem. 276*, 6125–6132.
27. Kamp, C., Silakov, A., Winkler, M., Reijerse, E. J., Lubitz, W, and Happe, T. (2008) Isolation and first EPR characterization of the [FeFe]-hydrogenases from green algae. *Biochim. Biophys. Acta 1777*, 410–416.
28. Girbal, L., von Abendroth, G., Winkler, M., Benton, P. M., Meynial-Salles, I., Croux, C., Peters, J. W., Happe, T., and Soucaille, P. (2005) Homologous and heterologous overexpression in *Clostridium acetobutylicum* and characterization of purified clostridial and algal Fe-only hydrogenases with high specific activities. *Appl. Environ. Microbiol. 71*, 2777–2781.
29. Dau, H., Liebisch, P., and Haumann, M. (2003) X-ray absorption spectroscopy to analyze nuclear geometry and electronic structure of biological metal centers-potential and questions examined with special focus on the tetra-nuclear manganese complex of oxygenic photosynthesis. *Anal. Bioanal. Chem. 376*, 562–583.
30. von Abendroth, G., Stripp, S., Silakov, A., Croux, C., Soucaillec, P., Girbal, L., and Happe, T. (2008) Optimized over-expression of [FeFe] hydrogenases with high specific activity in *Clostridium acetobutylicum*. *Int. J. Hydrogen Energy 33*, 6076–6081.
31. Wiesenborn, D. P., Rudolph, F. B., and Papoutsakis, E. T. (1988) Thiolase from *Clostridium acetobutylicum* ATCC 824 and its role in the synthesis of acids and solvents. *Appl. Environ. Microbiol. 54*, 2717–2722.
32. Barra, M., Haumann, M., Loja, P., Krivanek, R., Grundmeier, A., and Dau, H. (2006) Intermediates in assembly by photoactivation after heat-induced disassembly of the manganese complex of photosynthetic water oxidation. *Biochemistry 45*, 14523–14532.
33. Schäfers, F., Mertin, M., and Gorgoi, M. (2007) KMC-1: a high resolution and high flux soft x-ray beamline at BESSY. *Rev. Sci. Instrum. 78*, 1–14.
34. Dau, H., Liebisch, P., and Haumann, M. (2004) The structure of the manganese complex of photosystem II in its dark-stable S_1-state: EXAFS results in relation to recent crystallographic data. *Phys. Chem. Chem. Phys. 6*, 4781–4792.
35. Tomic, S., Searle, B. G., Wander, A., Harrison, M. N., Dent, A. J., Mosselmans, J. F. W., and Inglesfield, J. E. (2005) New tools for the analysis of EXAFS: The DL_EXCURV package, CCLRC Technical Report DL-TR-2005-001, ISSN 1362-0207.
36. Klementiev, K. V. (2005) XANES dactyloscope for Windows, freeware: www.desy.de/~klmn/xanda.html.
37. Gu, W., Jacquamet, L., Patil, D. S., Wang, H. X., Evans, D. J., Smith, M. C., Millar, M., Koch, S., Eichhorn, D. M., Latimer, M., and Cramer, S. P. (2003) Refinement of the nickel site structure in *Desulfovibrio gigas* hydrogenase using range-extended EXAFS spectroscopy. *J. Inorg. Biochem. 93*, 41–51.
38. Löscher, S., Burgdorf, T., Zebger, I., Hildebrandt, P., Dau, H., Friedrich, B., and Haumann, M. (2006) Bias from H_2 cleavage to production and coordination changes at the Ni-Fe active site in the NAD^+-reducing hydrogenase from *Ralstonia eutropha*. *Biochemistry 45*, 11658–11665.
39. Zabinsky, S. I., Rehr, J. J., Aukudinov, A., Albers, R. C., and Eller, M. J. (1995) Multiple-scattering calculations of x-ray-absorption spectra. *Phys. Rev. B 52*, 2995–3009.
40. Westre, T. E., Kennepohl, P., DeWitt, J. G., Hedman, B., Hodgson, K. O., and Solomon, E. I. (1997) A multiplet analysis of the Fe K-edge 1s→3d pre-edge features of iron complexes. *J. Am. Chem. Soc. 119*, 6297–6314.
41. Lemon, B. J., and Peters, J. W. (1999) Binding of exogenously added carbon monoxide at the active site of the iron-only hydrogenase (CpI) from *Clostridium pasteurianum*. *Biochemistry 38*, 12969–12973.
42. De Lacey, A., Stadler, C., Cavazza, C., Hatchikian, E. C., and Fernandez, V. M. (2000) FTIR characterization of the active site of the Fe-hydrogenase from *Desulfovibrio desulfuricans*. *J. Am. Chem. Soc. 122*, 11232–11233.
43. Tye, J. W., Darensbourg, M. Y., and Hall, M. B. (2008) Refining the active site structure of iron-iron hydrogenase using computational infrared spectroscopy. *Inorg. Chem. 47*, 2380–2388.
44. Pandey, A. S., Harris, T. V., Giles, L. J., Peters, J. W., and Szilagyi, R. K. (2008) Dithiomethylether as a ligand in the hydrogenase H-cluster. *J. Am. Chem. Soc. 130*, 4533–4540.
45. Fan, H.-J., and Hall, M. B. (2001) A capable bridging ligand for Fe-only hydrogenase: density functional calculations of a low-energy route for heterolytic cleavage and formation of dihydrogen. *J. Am. Chem. Soc. 123*, 3828–3829.

46. Schwartz, L., Eilers, G., Eriksson, L., Gogoll, A., Lomoth, R., and Ott, S. (2006) Iron hydrogenase active site mimic holding a proton and a hydride. *Chem. Commun. 2006*, 520–522.
47. Henry, R. M., Shoemaker, R. K., DuBois, D. L., and DuBois, M. R. (2006) Pendant bases as proton relays in iron hydride and dihydrogen complexes. *J. Am. Chem. Soc. 128*, 3002–3010.
48. Popescu, V. C., and Münck, E. (1999) Electronic structure of the H cluster in [Fe]-hydrogenases. *J. Am. Chem. Soc. 121*, 7877–7884.
49. Albracht, S. P. J., Roseboom, W, and Hatchikian, E. C. (2006) The active site of the [FeFe]-hydrogenase from *Desulfovibrio desulfuricans*. I. Light sensitivity and magnetic hyperfine interactions as observed by electron paramagnetic resonance. *J. Biol. Inorg. Chem. 11*, 88–101.
50. Voevodskaya, N., Lendzian, F., Sanganas, O., Grundmeier, A., Gräslund, A., and Haumann, M. (2008) Characterization of redox intermediates of the O_2-activating Mn-Fe site in R2 protein of *Chlamydia trachomatis* ribonucleotide reductase by X-ray absorption spectroscopy and EPR. *J. Biol. Chem.* (Epub doi:10.1074/jbc. M807190200).
51. Silakov, A., Reijerse, E. J., Albracht, S. P. J., Hatchikian, E. C., and Lubitz, W. (2007) The electronic structure of the H-cluster in the [FeFe]-hydrogenase from *Desulfovibrio desulfuricans*: A Q-band ^{57}Fe-ENDOR and HYSCORE study. *J. Am. Chem. Soc. 129*, 11447–11458.
52. Strange, R. W., and Feiters, M. C. (2008) Biological X-ray absorption spectroscopy (BioXAS): a valuable tool for the study of trace elements in the life sciences. *Curr. Opin. Struct. Biol. 18*, 609–616.
53. Haumann, M., Liebisch, P., Müller, C., Barra, M., Grabolle, M., and Dau, H. (2005) Photosynthetic O_2 formation tracked by time-resolved x-ray experiments. *Science 310*, 1019–1021.
54. Kleifeld, O., Frenkel, A., Martin, J. M. L., and Sagi, I. (2003) Active site electronic structure and dynamics during metalloenzyme catalysis. *Nat. Struct. Biol. 10*, 98–103.
55. Haumann, M., Grundmeier, A., Zaharieva, I., and Dau, H. (2008) Photosynthetic water oxidation at elevated dioxygen partial pressure monitored by time-resolved X-ray absorption measurements. *Proc. Natl. Acad. Sci. U.S.A. 105*, 17384–17389.
56. Sommerhalter, M., Lieberman, R. L., and Rosenzweig, A. C. (2005) X-ray crystallography and biological metal centers: is seeing believing?. *Inorg. Chem. 44*, 770–778.
57. Fiedler, A. T., and Brunold, T. C. (2005) Computational studies of the H-cluster of Fe-only hydrogenases: geometric, electronic, and magnetic properties and their dependence on the [Fe4S4] cubane. *Inorg. Chem. 44*, 9322–9334.
58. Liu, Z. P., and Hu, P. (2002) A density functional theory study on the active center of Fe-only hydrogenase: characterization and electronic structure of the redox states. *J. Am. Chem. Soc. 124*, 5175–5182.
59. Bruschi, M., Fantucci, P., and De Gioia, L. (2003) Density functional theory investigation of the active site of [Fe]-hydrogenases: effects of redox state and ligand characteristics on structural, electronic, and reactivity properties of complexes related to the [2Fe]H subcluster. *Inorg. Chem. 42*, 4773–4781.
60. Glatzel, P., and Bergmann, U. (2005) High resolution 1s core hole X-ray spectroscopy in 3d transition metal complexes—electronic and structural information. *Coord. Chem. Rev. 249*, 65–95.
61. Lawrence, J. D., Li, H., Rauchfuss, T. B., Benard, M., and Rohmer, M. M. (2001) Diiron azadithiolates as models for the iron-only hydrogenase active site: Synthesis, structure, and stereoelectronics. *Angew. Chem., Int. Ed. 40*, 1768–1771.
62. Beinert, H., Holm, R. H., and Münck, E. (1997) Iron-sulfur clusters: Nature's modular, multipurpose structures. *Science 277*, 653–659.
63. Imlay, J. A. (2006) Iron-sulphur clusters and the problem with oxygen. *Mol. Microbiol. 59*, 1073–1082.